J. Fluid Mech. (1967), *vol.* 30, *part* 3, *pp.* 547–560
Printed in Great Britain

Two-dimensional turbulent wakes

By IAN S. GARTSHORE
Department of Mechanical Engineering, McGill University

(Received 16 November 1966 and in revised form 21 July 1967)

The equations of mean motion indicate that two-dimensional turbulent wakes, when subjected to appropriately tailored adverse pressure gradients, can be self-preserving. An experimental examination of two nearly self-preserving wakes is reported here. Mean velocity, longitudinal and lateral turbulence intensity, intermittency and shear stress distributions have been measured and are compared with Townsend's data from the small-deficit undistorted wake. In comparison with the undistorted case, the present wakes have slightly lower turbulent intensities and significantly lower shear stresses, all quantities being non-dimensionalized by a local velocity scale taken as the maximum mean velocity deficit. A consideration of the reasons for the shear stress reduction leads to an expression from which the shear stresses in any symmetrical free equilibrium shear flow can be found. This relationship is used to calculate the rate of growth in the measured wakes, with reasonable success.

1. Introduction

Until recently, all experimental evidence for shear flows indicated that a self-preserving flow occurs in any situation for which a self-preserving form of the equation of mean motion can be written. Reynolds (1962) and Keffer (1965) have shown, however, that further conditions must be satisfied. They examined wakes subjected to approximately uniform and constant rates of strain and found that, despite the existence of a self-preserving form of the equation of mean motion, their flows were seldom if ever self-preserving. This result was attributed by both authors to a production of turbulent energy dependent on the applied uniform rate of strain and not on the local shear stress. Through this production term, it appears that the precise form of distortion creating the wake can influence the entire flow development whereas the details of the initial distortion are irrelevant in a truly self-preserving motion.

Since self-preserving flows are of particular importance in the study of turbulent shear, because of their relative simplicity, it is of interest to examine other potentially self-preserving wakes developing in appropriately tailored distortions. This paper describes an experimental study of two such two-dimensional wakes and discusses the relationships between simple free turbulent self-preserving shear flows. For completeness, the conditions specified by the equations of mean motion for self-preservation will be described before presenting the experimental results.

2. The conditions for self preservation

Following Townsend (1956*a*) and Patel & Newman (1961), a shear flow is considered whose mean properties are functions of x and y only and which is always confined to a sufficiently narrow region that the 'boundary-layer' approximations apply. The equation of motion in the x direction may then be written as

$$U\frac{\partial U}{\partial x}+V\frac{\partial U}{\partial y}+\frac{\partial \overline{uv}}{\partial y}+\frac{\partial}{\partial x}(\overline{u^2}-\overline{v^2})=U_1\frac{dU_1}{dx}+\nu\frac{\partial^2 U}{\partial y^2}, \tag{1}$$

where U_1 is the free-stream velocity outside the shear flow.

Assuming self preservation, and using Townsend's notation, the velocity scale U_0 and length scale L_0 are introduced by means of the following functional relationships:

$$\left.\begin{aligned} U &= U_1+U_0 f(\eta),\\ \overline{u^2} &= U_0^2 g_1(\eta),\\ \overline{v^2} &= U_0^2 g_2(\eta),\\ \overline{uv} &= U_0^2 g_{12}(\eta), \end{aligned}\right\} \tag{2}$$

where $\eta=(y/L_0)$. The scale U_0 may be conveniently defined in wakes as the maximum velocity deficit and for jets as the maximum velocity increment; the length scale L_0 is taken in this discussion as half the width between positions of half maximum velocity deficit of the wake or jet mean velocity profile.

With the continuity equation for the mean flow, and the forms given by (2), the equation of motion becomes

$$\begin{aligned} &\frac{d}{dx}(U_0U_1)f+U_0\frac{dU_0}{dx}\{2(g_1-g_2)+f^2\}-\frac{U_0}{L_0}\frac{d(L_0U_1)}{dx}\eta f'\\ &\qquad-\frac{U_0}{L_0}\frac{d}{dx}(L_0U_0)f'\int_0^\eta f\,d\eta-\frac{U_0^2}{L_0}\eta(g_1'-g_2')\frac{dL_0}{dx}\\ &\qquad+\frac{U_0^2}{L_0}g_{12}'=\frac{\nu U_0}{L_0^2}f'', \end{aligned} \tag{3}$$

where primes indicate differentiation with respect to η.

For self preservation, the x-dependent coefficients of the terms in (3) must be proportional to one another, or constants, so that (if the viscous term can be neglected) the following parameters must be independent of x:

$$\frac{L_0}{U_0^2}\frac{d(U_0U_1)}{dx};\quad \frac{L_0}{U_0}\frac{dU_0}{dx};\quad \frac{1}{U_0}\frac{d(L_0U_1)}{dx};\quad \frac{1}{U_0}\frac{d(L_0U_0)}{dx};\quad \frac{dL_0}{dx}.$$

These requirements are satisfied if

$$\left.\begin{aligned} L_0 &\propto (x+x_0),\\ U_0 &\propto (x+x_0)^{-1/m},\\ U_1 &\propto (x+x_0)^{-1/m}, \end{aligned}\right\} \tag{4}$$

where x_0 and m are constants for a particular flow. Another possibility, that L_0 is constant, is not of interest here.

Since U_0/U_1 is a constant, a rather simple form of the momentum integral equation may be written, using the functional forms defined in (2). The complete integral equation is

$$U_1^a \frac{U_0}{U_1} L_0 \left\{ \int_0^\infty f d\eta + \frac{U_0}{U_1} \int_0^\infty f^2 d\eta + \int_0^\infty (g_1 - g_2) d\eta \right\} = \text{constant},$$

where

$$a = 2 + \frac{\int_0^\infty f d\eta}{\int_0^\infty (f + g_1 - g_2) d\eta + \frac{U_0}{U_1} \int_0^\infty f^2 d\eta}, \tag{5}$$

which essentially imposes the additional condition that

$$U_1^a L_0 = \text{constant}. \tag{6}$$

The constant a, which is dependent on U_0/U_1 as shown in (5), must be equal to m by equations (4) and (6) so that the momentum integral equation merely defines the exponent m in terms of the ratio U_0/U_1.

In summary, the momentum equation implies, for a self-preserving two-dimensional shear flow, that the conditions in (4) are satisfied where m is equal to a, defined following (5). This analysis, which was given in almost the same form by Patel & Newman, applies equally well to jets or wakes provided U_0 and f are appropriately defined in each case. Since the shape of $f(\eta)$ changes little between jets and wakes, it is convenient to regard U_0 as positive for jets and negative for wakes.

Because g_1 and g_2 are positive functions and are small almost everywhere in comparison with f, the relation for a or m can usually be written with good accuracy as

$$\frac{1}{m-2} = 1 + \frac{U_0}{U_1} \frac{\int_0^\infty f^2 d\eta}{\int_0^\infty f d\eta}. \tag{7}$$

Three limiting values of m can be readily identified:

(i) $U_0 \to 0$; $m = 3$; the exactly self-preserving small-deficit wake (or small-increment jet);

(ii) $U_1 \to 0$; $m = 2$; the free jet in still air;

(iii) $U_0 = -U_1$; $m \approx 5{\cdot}4$; the wake having the largest possible velocity deficit but without backflow. The function $f(\eta)$ defined in (8) was used to evaluate m in this case.

3. An experimental study of two potentially self-preserving wakes

3.1 *Experimental arrangements*

The wake measurements described here were made in the McGill University open-circuit blower wind tunnel which has a rectangular working section of dimensions 17 in. × 30 in. Both 30 in. sides of the tunnel were replaced, for these experiments, by slats which could be adjusted to bleed air from the tunnel in

order to create an adverse pressure gradient when a perforated plate was fastened over the downstream end of the section. A $\frac{1}{4}$ in. square rod, attached to the mid-points of the 17 in. sides of the tunnel with one flat face normal to the oncoming stream, was used as the wake-forming body. The $\frac{1}{4}$ in. dimension is denoted in the text and figures by the symbol d.

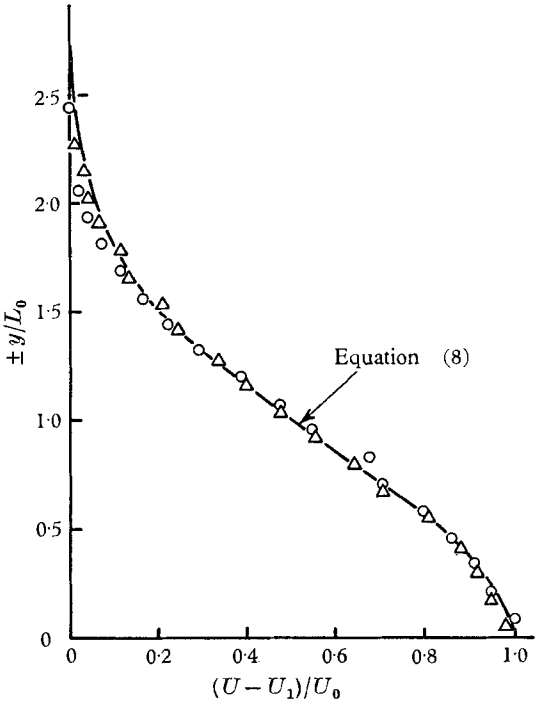

FIGURE 1. The mean velocity distribution for wake A. Streamwise location is $x/d = 194{\cdot}5$. ○, $y < 0$; △, $y > 0$.

Mean velocities were measured with a round Pitot tube having sharpened lips together with static taps located in one of the side walls. A DISA constant-temperature hot-wire anemometer was used to obtain measurements of turbulent quantities. Intermittency measurements were made by visual examination of trace recordings, as described previously (Gartshore 1965).

In forming the wakes, the pressure gradient downstream of the square rod was adjusted until an approximately constant ratio of U_0/U_1 was obtained. Final measurements of wake growth and external pressure gradient were then made. The two wakes formed in this way have been designated as wake A and wake B.

3.2. *The mean motion and external pressure gradient*

The non-dimensional profile of mean velocity in wake A is shown in figure 1, and within experimental error is the same as that in wake B. A convenient approximation to this distribution is given by

$$\begin{aligned} U_1 - U &= -U_0 \exp\left(-k(y/L_0)^2\right) \\ &= -U_0 f(\eta), \end{aligned} \tag{8}$$

where $k = \ln 2$ by definition of L_0. This curve is also plotted in figure 1. For values of (y/L_0) greater than about 1·5, the exponential curve slightly overestimates the actual mean velocity, which is the usual mode of departure.

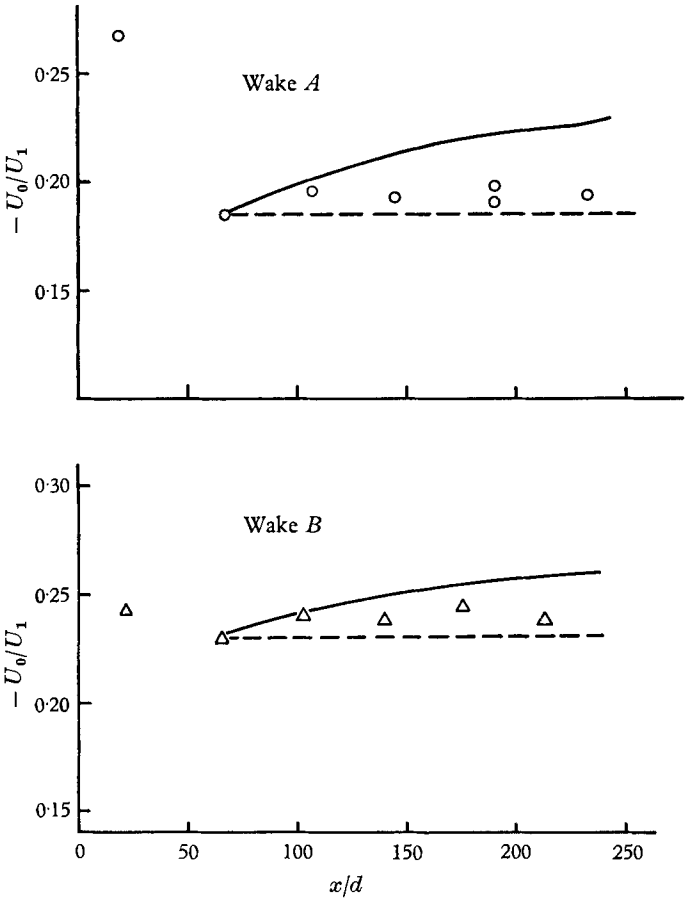

FIGURE 2. Mean-velocity deficit on wake centre-lines. △, ○, measured values; ——, calculated values using observed pressure gradient; – – –, calculated values using pressure gradient required for exact self preservation.

Streamwise distributions of the ratio U_0/U_1 are shown in figure 2 for the two wakes; both vary only slightly over the range investigated. Using average values of U_0/U_1 for each wake, theoretical values of m can be found for the two cases using (7) and (8); these are listed, together with other relevant data for the two wakes, in table 1.

The growth of each wake is plotted in figure 3, where L_0, the half-width to half-depth, is plotted against x. Approximate linearity is evident in conformity with the prediction of (4).

The measured external pressure distributions are plotted in figure 4 as U_1^{-m} against x (distance from the leading edge of the wake-forming body) for the two wakes. The parameter m has been calculated from (7) and from the mean experimentally measured value of U_0/U_1 on the assumption that (4) are a sufficiently

accurate description of the actual flow to permit a and m to be equated. Approximate linearity is evident in both cases, confirming the usefulness of (4).

One deficiency in the present measurements becomes evident from a close comparison of figures 3 and 4: the wake width L_0 and the external velocity parameter U_1^{-m} are both approximately linear but they have different virtual origins (i.e. values of x_0 in (4)). The wake B is considerably closer to true self preserva-

Wake A					Wake B				
$\frac{x}{d}$	$-\frac{U_0}{U_1}$	$\frac{L_0}{d}$	$\frac{U_1}{U_{1\,\mathrm{ref}}}$	C	$\frac{x}{d}$	$-\frac{U_0}{U_1}$	$\frac{L_0}{d}$	$\frac{U_1}{U_{1\,\mathrm{ref}}}$	C
21·2	0·266	1·72	1·14	—	22·7	0·243	1·82	1·22	—
72·2	0·184	4·14	1·00	1·00	66	0·230	3·98	1·00	1·00
112	0·194	4·94	0·92	0·906	104	0·241	5·18	0·91	0·957
149	0·192	5·52	0·89	0·860	140	0·239	6·06	0·88	1·00
194·5	0·196	6·44	0·84	0·816	176	0·244	6·80	0·84	0·992
237	0·192	7·22	0·80	0·775	213	0·238	7·32	0·82	0·992
Average U_0/U_1 is $-0{\cdot}192$					Average U_0/U_1 is $-0{\cdot}239$				
Mean m is 3·16					Mean m is 3·20				
At body $U_1 d/\nu = 6300$					At body $U_1 d/\nu = 7300$				

TABLE 1. C is $(U_1^m L_0)$ non-dimensionalized by the value of this quantity at the first measurement station at which the wake growth is linear

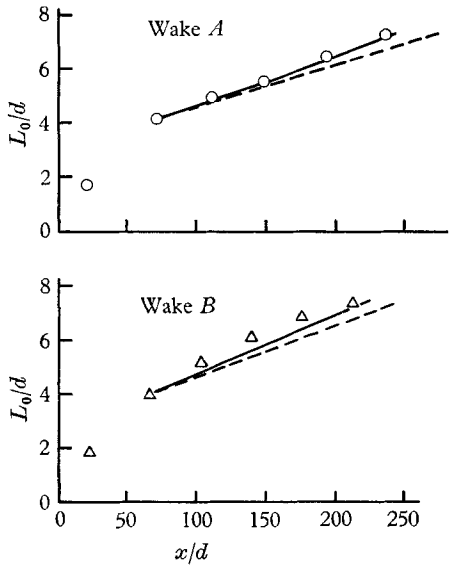

FIGURE 3

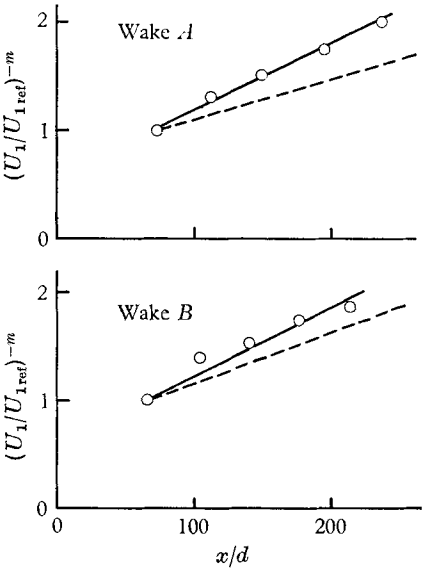

FIGURE 4

FIGURE 3. Wake widths. △, ○ measured values; ——, calculated values using observed pressure gradient; – – –, calculated values using pressure gradient required for exact self preservation.

FIGURE 4. Variation of external velocity. ○, measured values; ——, pressure gradient assumed in calculations based on observed values; – – –, pressure gradient required for exact self preservation.

tion in this regard, having values of x_0/d for the width and external velocity variations of about 92 and 86 respectively. Corresponding values of x_0/d for wake A are approximately 152 and 82.

A final check on the mean motion of the two wakes is possible through the use of (6), derived from the momentum integral condition. Values of $(U_1^m L_0)$, normalized by the value of the first measurement station, are listed in table 1. Wake A does not conform particularly well to (6), the 'constant' changing by over 20% for the total streamwise distance investigated. Such changes in experimentally determined momentum constants are unfortunately typical, being evident in the measurements of Townsend (1956*a*) and Reynolds (1962). Wake B agrees quite well with the requirement of (6).

From the mean velocity measurements, both wakes appear to be approximately self-preserving, wake B being more closely so than wake A. Attention will next be given to the turbulent intensity and shear distributions.

3.3. *Turbulent intensities and shear distributions*

The longitudinal turbulent intensity, non-dimensionalized with the velocity scale U_0, is plotted in figure 5 for wake A and in figure 6 for wake B. The effect of increasing $|U_0/U_1|$ (which is largest in wake B), is in general to lower the ratio $\overline{u^2}/U_0$. Based on the results of Townsend (1956*a*) for the zero-pressure-gradient case, it appears that the present wakes are very close to complete self preservation in the streamwise range $x/d > 140$.

The lateral turbulence intensity distributions, measured in wake A at $x/d = 194{\cdot}5$ and in wake B at $x/d = 140$, are plotted in figure 7, and compared there with zero-pressure-gradient results. Differences between the three results are surprisingly large near the wake centre-line but in general the figure shows that the effect of increasing the ratio $|U_0/U_1|$ is again to reduce the intensity ratio.

Distributions of shear stress in the two wakes are plotted in figure 8 together with results for the small-deficit, zero-pressure-gradient wake calculated from Townsend's measurements of mean velocity (1956*a*), and the equations of mean motion. (Incidentally, using Townsend's measured distribution of $\overline{u^2}$, and the present values of $\overline{uv}/U_0^2$ derived from his mean velocity measurements, a maximum shear coefficient $-\overline{uv}/\overline{u^2}$ of 0·62 can be found, considerably larger than the maximum value of 0·41 reported by Townsend for this flow.)

The present measurements of shear stress agree quite well with values calculated from the equations of motion and indicate large reductions in stress compared with the zero-pressure-gradient case. A slight decrease in stress is apparent from wake A to wake B as well, following the trend observed in the normal stress distributions for a lower intensity corresponding to a larger value of $|U_0/U_1|$.

For two-dimensional mean motion, the two turbulent energy production terms are

$$\overline{uv}\frac{\partial U}{\partial y} \quad \text{and} \quad (\overline{u^2}-\overline{v^2})\frac{\partial U}{\partial x}.$$

The second of these terms corresponds, for two-dimensional motion, to those found by Reynolds (1962) and Keffer (1965) to produce non-self-preserving

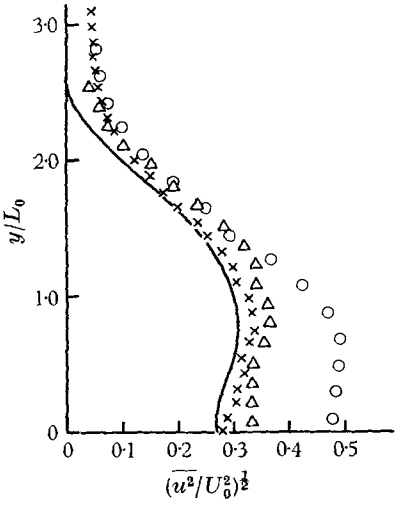

FIGURE 5

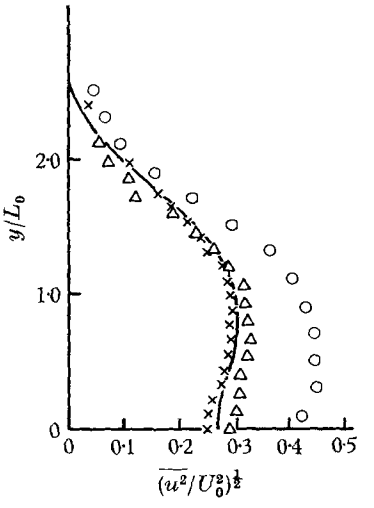

FIGURE 6

FIGURE 5. Longitudinal turbulence intensity ratio, wake A. ○, $x/d = 72$; △, $x/d = 149$; ×, $x/d = 237$; ——, zero-pressure-gradient, small-deficit wake, $x/d > 650$ (Townsend 1956*a*).

FIGURE 6. Longitudinal turbulence intensity ratio, wake B. ○, $x/d = 66$; △, $x/d = 140$; ×, $x/d = 213$; ——, zero-pressure-gradient, small-deficit wake, $x/d > 650$ (Townsend 1956*a*).

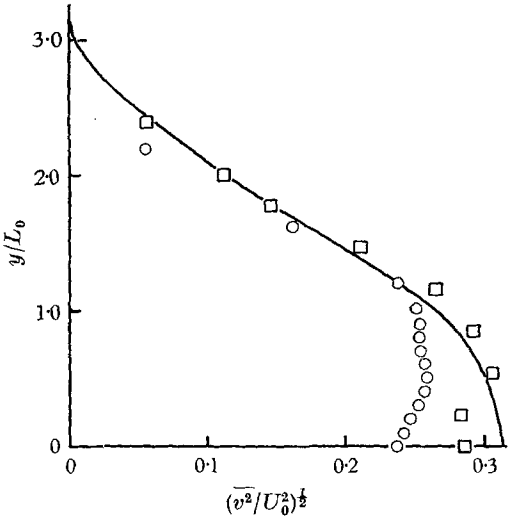

FIGURE 7

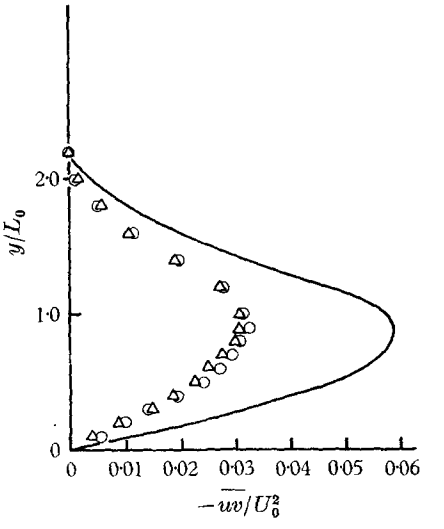

FIGURE 8

FIGURE 7. Lateral turbulence intensity ratio, wakes A and B. □, $x/d = 194{\cdot}5$, wake A; ○, $x/d = 140$, wake B; ——, zero-pressure-gradient, small-deficit wake, $x/d > 500$ (Townsend 1956*a*).

FIGURE 8. Shear stress distributions, wakes A and B. ○, $x/d = 194{\cdot}5$, wake A; △, $x/d = 140$, wake B; ——, zero-pressure-gradient, small-deficit wake, calculated from mean velocity measurements (Townsend 1956*a*) $x/d > 500$, using equations of mean motion.

motions in their distorted wakes, as described in § 1. A convenient measure of the relative importance of these two production terms in the present cases is, following Reynolds (1962), the parameter G defined as

$$G = \left[\frac{\overline{uv}}{\overline{u^2} - \overline{v^2}} \frac{\partial U/\partial y}{\partial U/\partial x}\right]_{y=L_0}.$$

Large values of G (greater than about unity) would imply a wake dominated by shear, whereas small values of this parameter would reflect a non-self-preserving development. In both the present wakes, the values of G are greater than 10 for typical streamwise positions ($x/d \approx 150$), so that their developments are dictated by the shear term in contrast to the wakes investigated by Keffer and Reynolds.

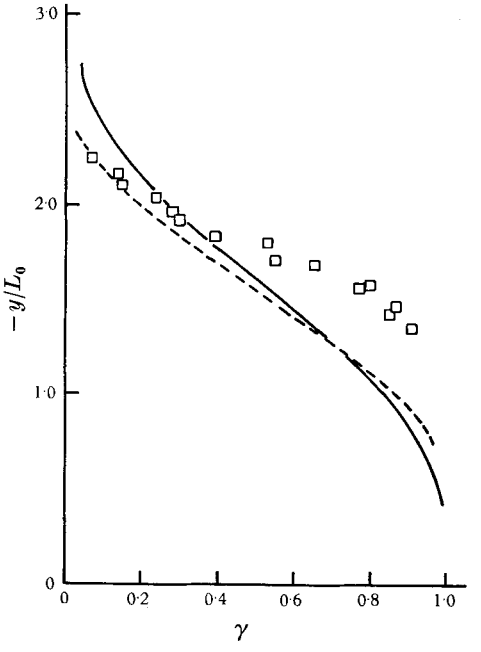

FIGURE 9. Intermittency distribution, wake B. □, measured values at $x/d = 140$; ——, small-deficit wake (Townsend 1949), $x/d = 1000$; – – –, small-deficit wake (Townsend 1956*a*), $x/d = 160$.

3.4. *The intermittency distribution*

The intermittency distribution was measured for wake B at $x/d = 140$ by a visual examination of trace recordings made of the differentiated signal from a normal hot wire. The results are plotted in figure 9, together with Townsend's (1956*a*) measurements at the same approximate streamwise location, in the zero-pressure-gradient wake. The measured distributions may be used to calculate σ, the standard deviation of the viscous superlayer from its mean position, a quantity which is a measure of mean wrinkle amplitude of the laminar–turbulent interface. For the present wake, $\sigma/L_0 = 0{\cdot}34$, whereas for Townsend's measurements (at $x/d = 160$), $\sigma/L_0 \approx 0{\cdot}48$. For comparison, the parameter σ/L_0 has a

value of about 0·61 in a small-deficit zero-pressure-gradient wake at $x/d \approx 1000$ (Townsend 1949).

Present measured values of σ/L_0 and R_T (defined following (10); R_T is essentially a non-dimensional representation of the turbulent shear stress at $y = L_0$) do not agree particularly well with a previous semi-empirical correlation of these two quantities presented by the present author (Gartshore 1965). One explanation for this lack of agreement is that there are, near a bluff wake-forming body, turbulent motions which contribute little to the shear stress. Considering the large turbulence production near a bluff body during the initial distortion, the presence of some largely irrelevant motions is not unlikely. The value of σ/L_0 measured by Townsend near a wake-forming body in zero pressure gradient is considerably smaller than the value of this quantity farther downstream, as noted above. The present value of σ/L_0 is consistent with Townsend's observations in so far as the value of σ/L_0 measured for wake B is too small for good agreement with the previously formulated correlation.

4. The effect of a small lateral strain

Townsend (1956*a*) suggested that a positive lateral rate of strain $(\partial U/\partial x) > 0$ in a two-dimensional shear flow decreases the size of the largest eddies, thereby reducing the mixing and the effective shearing stresses. From his explanation it would appear that a negative lateral rate of strain would tend to increase the stresses, by increasing the large-eddy size. The present experiments, in which $(\partial U/\partial x)_{y=L_0} < 0$, show, however, that a negative lateral rate of strain again reduces the effective stresses, at least in so far as $(\partial U/\partial x)$ is typified by its value at $y = L_0$. An explanation of the effect of $(\partial U/\partial x)$ on the large eddies is presented below. It postulates the existence of a large eddy similar to that proposed by Townsend despite the fact that the details of Townsend's large-eddy structure have been shown to be inaccurate (Grant 1958). For the present heuristic purposes, these details are unimportant.

Physically the effect of a lateral rate of strain on a large eddy may be demonstrated by considering a very simple two-dimensional shear flow in which $\partial U/\partial y$ and $\partial U/\partial x$ are constant everywhere. Such a flow could be described by the stream function $\psi = Ay^2/2 + Bxy$ where $A = \partial U/\partial y$ and $B = \partial U/\partial x$. Two cases will be compared, $B > 0$ and $B < 0$, both having equal positive values of A. A small element of vorticity representing a large eddy and placed along the y-axis at $x = y = 0$ in the assumed flow will be rotated by the flow until it lies along the line $y = 0$, if $B > 0$ or along the line $y/x = -2B/A$ if $B < 0$. Meanwhile its vorticity will be stretched by the rate of strain field whose larger principal rate of strain direction makes an angle θ with the x-axis, where θ is given by

$$\theta = \tan^{-1}\left\{-\frac{2B}{A} + \left(4\frac{B^2}{A^2} + 1\right)^{\frac{1}{2}}\right\}$$

$$\approx \frac{\pi}{4} - \frac{B}{A} \quad \text{for} \quad |B/A| \ll 1.$$

The effect of the rates of strain on the small element of vorticity may be simply described by the angle between the element's final orientation (near which it spends most of its life) and the larger principal rate of strain direction. For both positive and negative B, this angle (denoted by β) is equal to $(\frac{1}{4}\pi - |B/A|)$, again for small $|B/A|$. Because the angle β is largest when $B = 0$, assuming a given value of A, the large-eddy vorticity in this case will be stretched less than for any other value of B. Since the lateral scale of an eddy is decreased by longitudinal stretching (assuming for this discussion that the effects of diffusion are minor), the large eddies in a flow in which $B = 0$ will be larger laterally than in any other case.

Although the present explanation of the way in which non-zero $(\partial U/\partial x)$ affects the large-eddy growth is somewhat different from that presented by Townsend (1956*a*), the present conclusions substantiate Townsend's hypothesis that the large eddies in a small-deficit wake in zero pressure gradient, in which $B \approx 0$, occupy a larger proportion of the mean flow shear region than in any other case. The expression for β above indicates that there is no effect on the large eddy of a change in sign of B, a conclusion which is unaffected by altering the sign of A, as may easily be shown by arguments similar to those used above.

5. A relation between approximately self-preserving flows

The previous section extended a suggestion by Townsend concerning the way in which the large eddies are modified by a lateral rate of strain. This led to the use of a parameter (B/A) representing the effect of this lateral strain rate, and, from physical arguments, to the conclusion that the sign of B is unimportant. This conclusion is used in the following paragraphs, to provide an empirical relation with which the growth of any approximately self-preserving symmetrical shear flow can be calculated.

The large-eddy energy equilibrium hypothesis may be expressed, for shear flows with similar profiles, as

$$\left(\frac{L_0}{l}\right)^2 \propto \left\{-\frac{U_0 L_0}{\overline{uv}}\left(\frac{\partial U}{\partial y}\right)\right\}_{y=L_0}, \tag{9}$$

where l is a length scale representative of the largest eddies in the flow, and the ordinate $y = L_0$ has been chosen for evaluation of the shear stress parameter (essentially a turbulent Reynolds number) on the assumption that this location is typical of the structure in the outer region of the flow. A derivation of (9), and some experimental results supporting it, were presented in a previous paper (Gartshore 1965).

The significance of a lateral strain rate may be assessed through the ratio $(\partial U/\partial x)/(\partial U/\partial y)$, measured at a non-dimensional ordinate typical of conditions affecting the large eddies, in this case the ordinate $y = L_0$. This ratio is analogous to the parameter (B/A) used in the discussion of the previous section. Denoting the ratio of the real rates of strain by ξ, then

$$\frac{l}{L_0} = h_1(\xi), \quad \text{where} \quad \xi = \left\{\frac{\partial U/\partial x}{\partial U/\partial y}\right\}_{y=L_0};$$

or, by (9),
$$R_T = h_2(\xi), \tag{10}$$

where
$$R_T = \left\{\frac{U_0 L_0}{\overline{uv}}\frac{\partial U}{\partial y}\right\}_{y=L_0}$$
$$= \left\{-\frac{kU_0^2}{\overline{uv}}\right\}_{y=L_0} \quad \text{using (8).}$$

From the arguments of the previous section, that the sign of B/A (and, by analogy, of ξ) is unimportant, the function h_2 must be even in ξ. Figure 10 shows the values of R_T and ξ evaluated experimentally in the two wakes A and B of §3 and also contains values obtained from measurements in two other exactly or approximately self-preserving cases: the small-deficit wake in zero pressure gradient, and the jet in still air. The values of R_T and ξ used for these last two

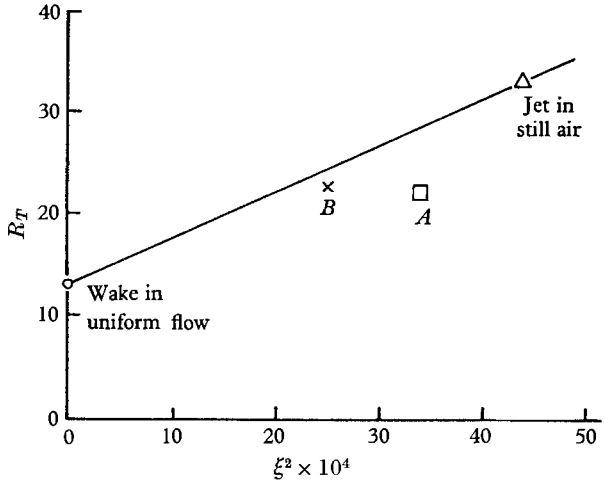

FIGURE 10. Comparison between four approximately self-preserving flows. ○, small-deficit wake in zero pressure gradient; △, two-dimensional jet in still surroundings; □, wake A, $x/d = 194{\cdot}5$, ×, wake B, $x/d = 140$; ——, equation (11).

cases are those given by Newman (1965) and are, jet: $R_T = 32{\cdot}9$, $\xi = 0{\cdot}0665$; wake: $R_T = 13{\cdot}0$, $\xi = 0$. The values of ξ for wakes A and B were obtained from the measured velocity and width variations, a process which involves differentiation of experimental results and is therefore somewhat inaccurate. Values of R_T for the present cases were obtained from the measured values of $(\overline{uv}/U_0^2)$ shown in figure 8.

The results presented in figure 10 are taken from quite different types of flows: the small-deficit zero-pressure-gradient wake is not exactly self-preserving and does not grow linearly, the jet in still air has a large positive value of $(\partial U/\partial x)_{L_0}$, whereas the wakes A and B have negative values of this parameter. Nevertheless, bearing in mind that wake B is more nearly two-dimensional and self-preserving than wake A, the function linking R_T and ξ for all cases appears to be representable by the simple relation

$$\left.\begin{aligned} R_T &= a_0 + a_1\xi^2, \\ \text{with} \quad a_0 &= 13 \quad \text{and} \quad a_1 = 4500. \end{aligned}\right\} \tag{11}$$

It is of practical engineering interest to see how accurately the approximate relation of (11) is able to predict the growth in width and the decay of velocity defect of the wakes A and B. For this purpose, two momentum integrals can be written, one extending across the entire flow and a second having limits $y = 0$ and $y = L_0$ which, with the velocity profile of (8), yield two total differential equations. A third equation describing the observed variation of external velocity was used (see figure 4) and the three equations were solved numerically using a Runge–Kutta integration scheme. The shear stress at $y = L_0$ in the flow is known from (11) and, except for the use of this equation, the method of calculation is not restricted to self-preserving cases.

The results of the calculations using the observed pressure gradients are shown in figures 2 and 3 together with the measured data. The agreement between measured and calculated values suggests that, for many purposes, (11) is sufficiently accurate to predict the streamwise development of symmetrical flows which are approximately self-preserving.

As already mentioned, the measured values of L_0 have different virtual origins from the corresponding variations of external velocity, a fact which explains the deviations of the calculated values of U_0/U_1 from a constant value and of the calculated growths of L_0 from precise linearity. The external velocity variation which would be required for exact self-preservation may be found from the two momentum integral equations already described, together with (11), simply by assuming that equations (4) are exact. The self-preserving development calculated in this way is plotted in figures 2 and 3 (again using the first experimental point to specify initial conditions) and the calculated external velocity variation required to produce this exact self preservation is shown in figure 4.

From the foregoing calculations, it is clear that a knowledge of the shear stress such as that postulated in (11) can be used either to predict the exact pressure variation required for a true self-preserving development or to predict the actual streamwise development of a nearly self-preserving flow when a measured pressure distribution is specified. How far an actual flow can deviate from exactly self-preserving conditions and still have its development predicted by (11) remains an open question however.

6. Other shear flows

Since the shear stress in a shear flow is governed primarily by the local scale of the large eddies, which is in turn affected by the mean rates of strain acting on the large eddies throughout their lifetime, the use of local strain rates will be appropriate only in self-preserving cases. In other cases, upstream values of the strain ratio must be found which account for the history of strain rates imposed on the large eddies, the distance upstream depending on the rate at which the flow is deviating from self-preserving development and on the time taken by the large eddies to modify their scale in response to the changing rates of strain.

In contrast to the wakes discussed here, equilibrium boundary layers appear to contain large eddies which change very little in scale, relative to the boundary-layer thickness, over a significant range of equilibrium parameter. Evidence for

this is given by Bradshaw's measurements (Bradshaw 1966) in which the non-dimensional mixing lengths in three equilibrium boundary layers are almost identical, near the centres of the layers; as can be shown from (9), the calculated mixing length is really a measure of the large-eddy scale (Gartshore 1965). Bradshaw's measurements justify Townsend's assumption for equilibrium boundary layers (Townsend 1956*b*) that the non-dimensional large-eddy scale is not affected by mean pressure gradient, an assumption which produced reasonably good agreement with Clauser's (1956) measurements in equilibrium cases. The wall itself sharply bounds the lateral extent of the large eddies and this severe restriction probably accounts for the constancy of large-eddy scale.

The author would like to thank Dr B. G. Newman for many helpful discussions during the course of this investigation, which was supported financially by the Defence Research Board of Canada under grant number 9551-12.

REFERENCES

BRADSHAW, P. 1966 The turbulence structure of equilibrium boundary layers. *N.P.L. Aero. Rept.* no. 1184.

CLAUSER, F. M. 1956 The turbulent boundary layer. *Advances in Applied Mechanics*, vol. 4. New York: Academic Press.

GARTSHORE, I. S. 1965 An experimental examination of the large-eddy equilibrium hypothesis. *J. Fluid Mech.* **24**, 89.

GRANT, H. L. 1958 The large eddies of turbulent motion. *J. Fluid Mech.* **4**, 149.

KEFFER, J. F. 1965 The uniform distortion of a turbulent wake. *J. Fluid Mech.* **22**, 135.

NEWMAN, B. G. 1965 Turbulent jets and wakes in a pressure gradient. *Proc. G.M. Conference, Detroit.* Elsevier Publishing Co.

PATEL, R. P. & NEWMAN, B. G. 1961 Self-preserving, two-dimensional turbulent jets and wall jets in a moving stream. *McGill University, MERL Rept.* Ae 5.

REYNOLDS, A. J. 1962 Observations on distorted turbulent wakes. *J. Fluid Mech.* **13**, 333.

TOWNSEND, A. A. 1949 The fully developed turbulent wake of a circular cylinder. *Aust. J. Sci. Res.* **2**, 451.

TOWNSEND, A. A. 1956*a* *The Structure of Turbulent Shear Flow.* Cambridge University Press.

TOWNSEND, A. A. 1956*b* The properties of equilibrium boundary layers. *J. Fluid Mech.* **1**, 561.